GEOLOGY | THE GEOLOGICAL SOCIETY OF AMERICA®

https://doi.org/10.1130/G45974.1

Manuscript received 3 January 2019
Revised manuscript received 8 April 2019
Manuscript accepted 9 April 2019

Overestimation of threat from 100 Mt–class airbursts? High-pressure evidence from zircon in Libyan Desert Glass

Aaron J. Cavosie[1] and Christian Koeberl[2,3]

[1]Space Science and Technology Centre and The Institute for Geoscience Research, School of Earth and Planetary Science, Curtin University, Perth, Western Australia 6102, Australia

[2]Natural History Museum, Burgring 7, A-1010 Vienna, Austria

[3]Department of Lithospheric Research, University of Vienna, Althanstrase 14, A-1090 Vienna, Austria

ABSTRACT

Atmospheric airbursts over Russia at Chelyabinsk in 2013 and Tunguska in 1908 provide dramatic examples of hazards posed by near-Earth objects (NEOs). These two events produced 0.5 and 5 Mt of energy, respectively, which dramatically affected surface environments and, in the case of Chelyabinsk, injured humans. Enigmatic natural glasses have been cited as geologic evidence of the threat posed by large airbursts. Libyan Desert Glass (LDG) is a natural glass found in western Egypt that formed ~29 m.y. ago, however its origin is disputed; the two main formation hypotheses include melting by meteorite impact or melting by a large, 100 Mt–class airburst. High-temperature fusion occurs during both processes, however airbursts do not produce shocked minerals; airbursts generate overpressures at the level of thousands of pascals in the atmosphere, whereas crater-forming impacts generate shockwaves at the level of billions of pascals on the ground. Here we report the presence in LDG of granular zircon grains that are comprised of neoblasts that preserve systematic crystallographic orientation relations that uniquely form during reversion from reidite, a 30 GPa high-pressure $ZrSiO_4$ polymorph, back to zircon. Evidence of former reidite provides the first unequivocal substantiation that LDG was generated during an event that produced high-pressure shock waves; these results thus preclude an origin of LDG by airburst alone. Other glasses of disputed origin that contain zircon with evidence of former reidite, such as Australasian tektites, similarly were also likely made during crater-forming events. Public-policy discussions and planning to mitigate hazards from airbursts caused by NEOs are clearly warranted, but should be cautious about considering LDG or other glasses with evidence of high-pressure shock deformation as products of an airburst. At present, there are no confirmed examples of products from a 100 Mt–class airburst in the geologic record.

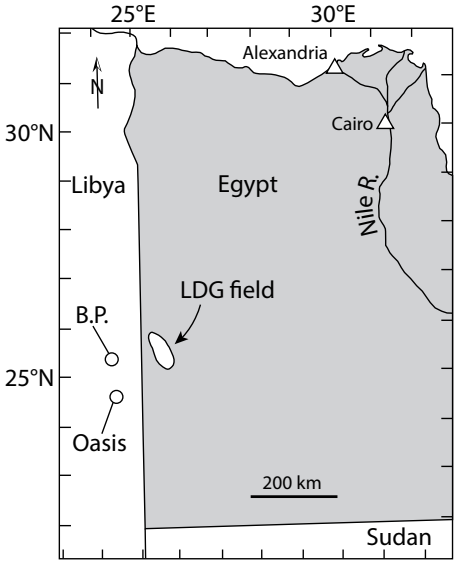

Figure 1. Map showing location of Libyan Desert Glass (LDG) field in western Egypt (after Koeberl, 1997). Also shown are two regional impact structures, B.P. (2 km diameter) and Oasis (18 km diameter) (Abate et al., 1999).

LIBYAN DESERT GLASS

Libyan Desert Glass (LDG) occurs over an area of several thousand square kilometers in the Great Sand Sea desert of western Egypt (Fig. 1). LDG consists of high-silica glass (>96 wt% SiO_2) that formed by fusion of a quartz-rich source ~29 m.y. ago (Koeberl, 1997). The ubiquitous presence of high-temperature products, including cristobalite, lechatelierite, and baddeleyite from dissociated zircon, and evidence of a meteoritic component (Koeberl, 2000) have lead many workers to argue that LDG originated by impact melting (e.g., Kleinmann, 1968; Koeberl, 1997; Fröhlich et al., 2013). However, no definitive links have been established between LDG and known impact structures in the region (Abate et al., 1999) (Fig. 1). Shocked minerals have not been identified in LDG, despite reports of shocked quartz in float (Kleinmann et al., 2001) and bedrock (Koeberl and Ferrière, 2019) samples of sandstone within the LDG field. In the absence of an identified source crater and any evidence of shock deformation within the glass, LDG has also been proposed to have formed as a consequence of a ~100 Mt (1 Mt = 4.184 × 10^{15} J) low-altitude atmospheric airburst, a process which would not generate shocked minerals or a crater, but would explain high-temperature fusion of surface materials (Wasson, 2003; Boslough and Crawford, 2008). Ascertaining the origin of LDG is critically important, as the interpretation of LDG as a product of airburst continues to inform U.S. government policy on hazards posed by near-Earth objects (NEOs) (e.g., Boslough, 2014; Boslough et al., 2015). Here we present the first quantitative orientation analysis of microstructures in zircon grains in LDG, all analyzed in situ within samples of the glass, which shows that some grains originated from the reversion of reidite, a high-pressure $ZrSiO_4$ polymorph. We then discuss the implications of these findings for hypotheses on the origin of LDG.

SAMPLES AND METHODS

Samples of LDG were collected by one of us (CK) during field work in western Egypt in 2003 and 2006. Seven different LDG samples were analyzed in this study, each mounted in epoxy.

CITATION: Cavosie, A.J., and Koeberl, C., 2019, Overestimation of threat from 100 Mt–class airbursts? High-pressure evidence from zircon in Libyan Desert Glass: Geology, https://doi.org/10.1130/G45974.1

The samples include typical characteristics of LDG described previously (e.g., Koeberl, 1997), including being generally translucent and yellow in color, and having variable dark- and/or light-colored wispy layering. Zircon grains in LDG samples were documented using backscattered electron (BSE) imaging with a scanning electron microscope. Orientation maps for zircon were collected using electron backscatter diffraction (EBSD) with step sizes ranging from 50 to 100 nm. Additional sample information and a full description of analytical methods are given in the GSA Data Repository[1].

RESULTS

Zircon Microstructures in LDG

Multiple zircon grains were found in each sample of LDG analyzed, and a total of 101 grains were documented. The majority of grains (65%) fully dissociated to zirconia (now baddeleyite) and are no longer zircon. The second-largest population of grains (24%) contain ubiquitous zirconia inclusions, and are interpreted to have fully dissociated to zirconia, and then partially or fully back-reacted with silica melt to form a new generation of zircon; the zirconia inclusions are preserved because they were isolated from further reaction with silica melt by newly formed zircon. As the aforementioned grains do not record information about their pre-dissociation history, they are not discussed further; representative BSE images of such grains are shown in the Data Repository (Item DR1). Only 11 of the 101 zircon grains (11%) showed no evidence of dissociation to zirconia, or in a few cases, only the margins of grains had dissociated (Item DR1). The 11 grains are composed of micrometer-sized neoblasts, and are the focus of this study.

Orientation analysis by EBSD was done on eight of the 11 granular grains (three were too small or inaccessible). In five of the grains, neoblast orientations are broadly dispersed, with minor variations, and they do not form discrete orientation clusters (Item DR1). In contrast, neoblasts in the other three grains occur in multiple orientation clusters with systematic relations. An example of a grain with systematic orientation clusters is shown in Figure 2. The grain has a granular zircon core consisting of 0.5–1.0 µm neoblasts, and a few zirconia inclusions located along the margin and/or along partings, both adjacent to glass (i.e., former melt) (Fig. 2A). The core is surrounded by a semi-detached rim that consists of ~0.5 µm zirconia grains (baddeleyite) that are enveloped by thin neoblastic overgrowths of zircon (Fig. 2A, inset). Orientation mapping reveals that the entirety of the grain consists of many distinct orientation clusters (Fig. 2B). However, zircon neoblasts comprising the granular core consist of only three mutually orthogonal orientation clusters that are highly systematic; each orientation cluster can be related to another cluster by 90°/<110> (Fig. 2C). High-angle (75°–95°) misorientation axes defined by adjacent neoblasts in the core are also highly systematic (Fig. 2D), and coincide with each of the three <110> clusters (Fig. 2C). In contrast, zircon in the rim consists of >15 orientation clusters, most of which do not preserve a systematic relation to each other or to neoblast clusters in the granular core (Item DR1). Baddeleyite grains enveloped by neoblastic zircon overgrowths in the rim are locally twinned (Item DR1).

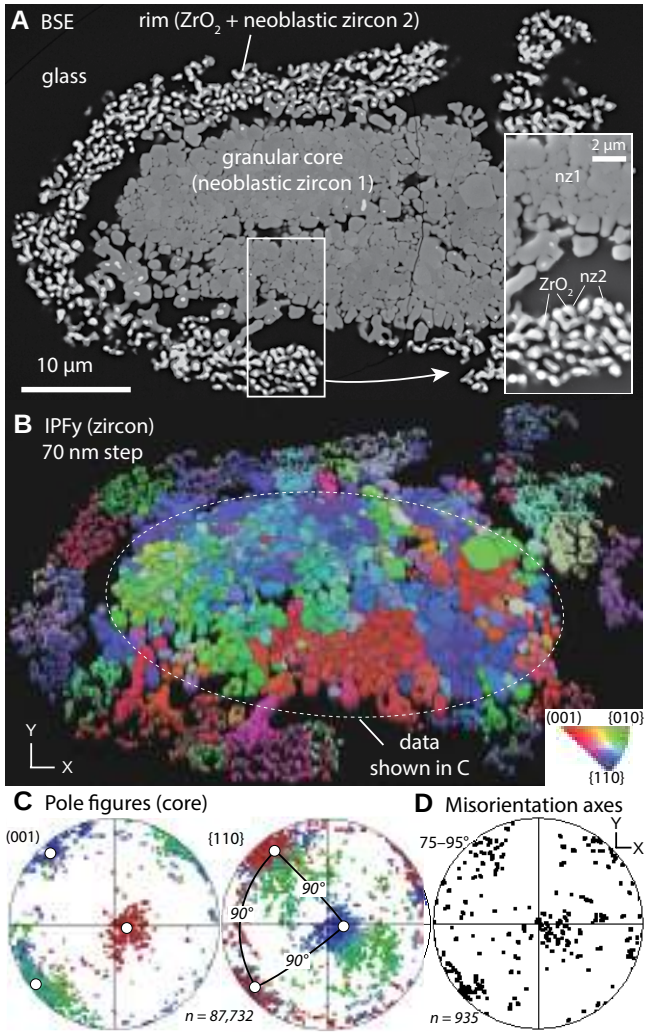

Figure 2. Granular zircon from Libyan Desert Glass that preserves evidence of former reidite. A: Backscattered electron (BSE) image showing granular core (neoblastic zircon 1, nz1) surrounded by partially detached corona (rim) consisting of zirconia (baddeleyite) intergrown with a later generation of neoblastic zircon (nz2). B: Orientation map shown with inverse pole figure (IPFy) color scheme. C: Pole figures showing data for granular zircon core (see oval in B). D: Plot showing high-angle (75°–95°) misorientation axes for data in C. Stereonets are equal-area, lower-hemisphere projections in sample *x-y-z* reference frame.

DISCUSSION

Pressure-Temperature History of LDG Recorded in Zircon Microstructures

The key to constraining formation conditions of LDG lies in deciphering the complex microstructural records of relict zircon entrained in the glass, due to its refractory nature and ability to survive total fusion of its host. Three populations of zircon were defined based on microstructure, with all three examples occurring within individual samples of LDG. These include: (1) zircon grains composed of granular neoblastic domains that did not dissociate (11%); such grains are the oldest generation of zircon preserved and in some cases provide constraints on pressure history; (2) dissociated zircon grains composed of baddeleyite (65%); such grains dominate the population and provide constraints on thermal history; and (3) dissociated grains that back-reacted with melt to form a second generation of neoblastic zircon (24%); such grains form during cooling, and do not record peak temperature or pressure conditions.

The zircon shown in Figure 2 is a granular grain that did not fully dissociate, and happens to contain domains representing each of the three different microstructures. It is therefore an ideal example for illustrating the chronological formation sequence of the various microstructures, from which a hypothetical pressure-temperature (*P-T*) path for LDG was constructed (Fig. 3).

[1]GSA Data Repository item 2019218, Item DR1 (additional information on samples), Item DR2 (additional information on methods), and Table DR1 (EBSD analytical conditions), is available online at http://www.geosociety.org/datarepository/2019/, or on request from editing@geosociety.org.

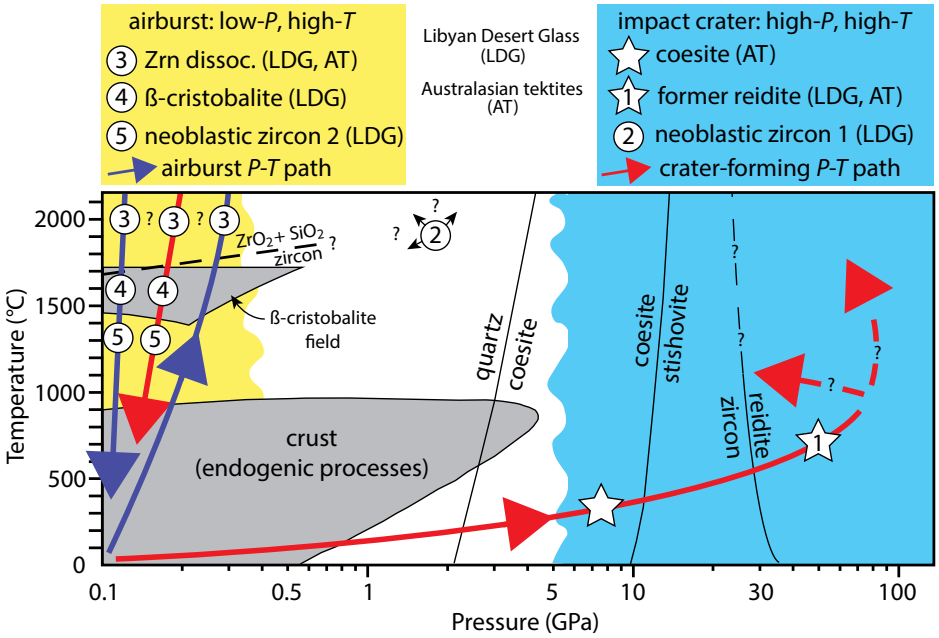

Figure 3. Simplified pressure-temperature (*P-T*) diagram (modified after French, 1998) showing hypothetical *P-T* paths for both airburst (purple) and crater-forming (red) events; dashed portions indicate different possible trajectories. Note that *P* indicated for airburst path is greatly exaggerated for convenience of illustration; atmospheric overpressures from airburst are in thousands of pascals range (e.g., Aftosmis et al., 2019). Observations from Libyan Desert Glass (LDG) (this study) and Australasian tektites (AT) (see text) are indicated. Neoblastic zircon 1 and 2 refer to different generations of zircon shown in Figure 2. "Reidite-in" and zircon dissociation (dissoc.) curves are from Timms et al. (2017). Cristobalite field is from Swamy et al. (1994).

The earliest events preserved are recorded in the granular neoblastic core (labeled nz1 in Fig. 2A, inset). The systematic 90°/<110> orientation relations for neoblast clusters in the core of the granular zircon (Figs. 2B and 2C), whereby each orientation cluster consists of both adjacent and dispersed (non-touching) neoblasts, form uniquely as a consequence of formation of the high-pressure $ZrSiO_4$ polymorph reidite, which occurs via 90°/<110> transformations (e.g., Cox et al., 2018), and its subsequent reversion back to zircon, which follows the same pathways (Erickson et al., 2017a; Timms et al., 2017). The former presence of reidite requires that some LDG zircon grains followed a *P-T* path that exceeded ~30 GPa (Kusaba et al., 1985; Leroux et al., 1999) (Fig. 3). Reidite is no longer present in any of the granular zircon grains; reversion of reidite and recrystallization into zircon neoblasts presumably occurred within the zircon stability field and below the zircon dissociation temperature, but the exact conditions are speculative (Fig. 3). In the five granular zircon grains analyzed that do not preserve systematic neoblast orientations (Item DR1), either reidite was absent, or the amount of reidite formed was minor enough to not significantly influence neoblast orientations.

The next event preserved is in the rim, which records dissociation of a ~5-µm-wide corona around the grain (Fig. 2A). The vast majority of LDG zircon grains documented in this study, 89/101 (89%), fully dissociated to zirconia, which has been shown in previous studies of single grains (Kleinmann, 1968; Fröhlich et al., 2013). Such grains provide unambiguous evidence for temperature >1687 °C, which is required for the dissociation of zircon to tetragonal zirconia + siliceous melt (Timms et al., 2017); the dissociation reaction is not well constrained at high pressure (Fig. 3), but appears to have a positive slope (Kleinmann, 1968; Timms et al., 2017). Tetragonal zirconia is no longer present, but is inferred to have existed based on ubiquitous reversion twins observed in baddeleyite (Item DR1), the monoclinic polymorph stable below 1175 °C (Timms et al., 2017). Dissociation of zircon is further consistent with the presence in LDG of α-cristobalite, a reversion product of β-cristobalite, a high-temperature, low-pressure silica polymorph that forms from 1726 to 1470 °C at <0.6 GPa (Swamy et al., 1994).

The third and final event recorded in LDG zircon grains consists of the growth of thin, neoblastic zircon films around zirconia grains in the rim (labeled nz2 in Fig. 2A, inset). This generation of zircon growth was likely facilitated by ingress of siliceous melt along and through the partially detached rim, where it reacted with zirconia to form a second generation of zircon. The thin zircon films must have formed in the zircon stability field during cooling, but prior to quenching of the melt to glass (Fig. 3).

Other Occurrences of Similar Granular Zircon

Granular zircon grains with the same neoblast orientation relations (e.g., orientation clusters defined by 90°/<110>) have been reported previously from confirmed impact structures and ejecta deposits, and are not known to form in other environments. Such granular zircon grains provide a quantitative means to identify the former presence of reidite, and have been termed "former reidite in granular neoblastic zircon", or FRIGN zircon (Cavosie et al., 2018a). So-called FRIGN zircon grains have been reported in impact glasses (Cavosie et al., 2016, 2018a, 2018b; Rochette et al., 2019) and also in partially devitrified impact melt rocks (Erickson et al., 2017b; Timms et al., 2017; Cavosie et al., 2018a; Kenny et al., 2019). The seven previously known occurrences of FRIGN zircon cited above highlight the ubiquitous involvement of both high-pressure shock deformation and high-temperature melting during its formation.

Reassessing Evidence of Airbursts in the Geological Record

Airbursts over Tunguska, Russia, in 1908 and Chelyabinsk, Russia, in 2013 are estimated to have released 5 Mt and 0.5 Mt of energy, respectively, to the near-surface environment (Brown et al., 2013), however melted or shock-deformed surface materials have not been reported from either location. The Tunguska event defines what is referred to as a type 1, ~5 Mt "Tunguska-class" airburst, formed by a ~20-m-diameter NEO (Boslough, 2014). In contrast, LDG has been used by some researchers to define the type example of the largest airburst known, a type 2, ~100 Mt "LDG-class" event, formed by a ~100-m-diameter NEO, where the fireball "…descends to the surface and expands radially, leading to incineration of organic material and melting of alluvium and surface rocks" (Boslough, 2014, p. 371). While evidence of high-temperature processes in LDG, including dissociated zircon, cristobalite, and mullite (Greshake et al., 2018), are consistent with formation of LDG on *P-T* paths characteristic of either a ~100 Mt–level airburst or crater formation (Fig. 3, left side), orientation data from granular zircon show that both LDG (this study) and Australasian tektites (Cavosie et al., 2018a) preserve evidence of former reidite, a >30 GPa polymorph of zircon. Formation of reidite in LDG and Australasian tektites, as well as other high-pressure phases in the latter (e.g., Walter, 1965), uniquely requires *P-T* paths that include high-pressure shock deformation, which only occurs during crater-forming events (Fig. 3, right side), rather than from airbursts (Wasson, 2003; Boslough and Crawford, 2008). Airburst events produce overpressures of thousands of pascals in the atmosphere, which, while capable of property damage and injury (e.g., Aftosmis

et al., 2019), are a factor of ~10^6 lower in pressure than that required to cause shock deformation (French, 1998). This observation may explain the disparity between the geological record and the predicted impact interval of ~100-m-diameter NEOs based on optical surveys (e.g., Boslough et al., 2015). Earth impacts with ~100-m-diameter NEOs, the size that could cause a ~100 Mt airburst, are predicted to occur every ~10^4 yr (e.g., Boslough et al., 2015). Thus, about 500 ~100-Mt-level (LDG-class) airbursts should have occurred over the last 5 m.y., whereas no confirmed airburst-related glass deposits from any size event are known from the geological record to have occurred in this time interval (cf. Schultz et al., 2006). Given the necessity of high-pressure shock deformation for formation of LDG and Australasian tektites, it can be concluded that no examples of ~100 Mt airburst events are currently known from the geological record, and thus NEO hazard mitigation policy should probably not consider the occurrence of LDG.

ACKNOWLEDGMENTS

Support was provided by the Space Science and Technology Centre, a Curtin Research Fellowship, and the Microscopy and Microanalysis Facility at Curtin University. We thank Dennis Brown for editorial handling, and Gavin Kenny and two anonymous reviewers for helpful reviews.

REFERENCES CITED

Abate, B., Koeberl, C., Kruger, F.J., and Underwood, J.R., Jr., 1999, BP and Oasis impact structures, Libya, and their relation to Libyan Desert Glass, *in* Dressler, B.O., and Sharpton, V.L., eds., Large Meteorite Impacts and Planetary Evolution II: Geological Society of America Special Paper 339, p. 177–192, https://doi.org/10.1130/0-8137-2339-6.177.

Aftosmis, M.J., Mathias, D.L., and Tarano, A.M., 2019, Simulation-based height of burst map for asteroid airburst damage prediction: Acta Astronautica, v. 156, p. 278–283, https://doi.org/10.1016/j.actaastro.2017.12.021.

Boslough, M., 2014, Airburst warning and response: Acta Astronautica, v. 103, p. 370–375, https://doi.org/10.1016/j.actaastro.2013.09.007.

Boslough, M.B.E., and Crawford, D.A., 2008, Low-altitude airbursts and the impact threat: International Journal of Impact Engineering, v. 35, p. 1441–1448, https://doi.org/10.1016/j.ijimpeng.2008.07.053.

Boslough, M., Brown, P., and Harris, A., 2015, Updated population and risk assessment for airbursts from near-Earth objects (NEOs): Paper presented at 2015 IEEE Aerospace Conference, Big Sky, Montana, USA, 7–14 March, 12 p., https://doi.org/10.1109/AERO.2015.7119288.

Brown, P.G., et al., 2013, A 500-kiloton airburst over Chelyabinsk and an enhanced hazard from small impactors: Nature, v. 503, p. 238–241, https://doi.org/10.1038/nature12741.

Cavosie, A.J., Timms, N.E., Erickson, T.M., Hagerty, J.J., and Hörz, F., 2016, Transformations to granular zircon revealed: Twinning, reidite, and ZrO_2 in shocked zircon from Meteor Crater (Arizona, USA): Geology, v. 44, p. 703–706, https://doi.org/10.1130/G38043.1.

Cavosie, A.J., Timms, N.E., Ferrière, L., and Rochette, P., 2018a, FRIGN zircon—The only terrestrial mineral diagnostic of high-pressure and high-temperature shock deformation: Geology, v. 46, p. 891–894, https://doi.org/10.1130/G45079.1.

Cavosie, A.J., Timms, N.E., Erickson, T.M., and Koeberl, C., 2018b, New clues from Earth's most elusive impact crater: Evidence of reidite in Australasian tektites from Thailand: Geology, v. 46, p. 203–206, https://doi.org/10.1130/G39711.1.

Cox, M.A., Cavosie, A.J., Bland, P.A., Miljković, K., and Wingate, M.T.D., 2018, Microstructural dynamics of central uplifts: Reidite offset by zircon twins at the Woodleigh impact structure, Australia: Geology, v. 46, p. 983–986, https://doi.org/10.1130/G45127.1.

Erickson, T.M., Pearce, M.A., Reddy, S.M., Timms, N.E., Cavosie, A.J., Bourdet, J., Rickard, W.D.A., and Nemchin, A.A., 2017a, Microstructural constraints on the mechanisms of the transformation to reidite in naturally shocked zircon: Contributions to Mineralogy and Petrology, v. 172, 6, https://doi.org/10.1007/s00410-016-1322-0.

Erickson, T.M., Timms, N.E., Kirkland, C.L., Tohver, E., Cavosie, A.J., Pearce, M.A., and Reddy, S.M., 2017b, Shocked monazite chronometry: Integrating microstructural and in situ isotopic age data for determining precise impact ages: Contributions to Mineralogy and Petrology, v. 172, 11, https://doi.org/10.1007/s00410-017-1328-2.

French, B.M., 1998, Traces of catastrophe: A handbook of shock-metamorphic effects in terrestrial meteorite impact structures: Houston, Texas, Lunar and Planetary Institute, 120 p.

Fröhlich, F., Poupeau, G., Badou, A., Le Bourdonnec, F.X., Sacquin, Y., Dubernet, S., Bardintzeff, J.M., Véran, M., Smith, D.C., and Diemer, E., 2013, Libyan Desert Glass: New field and Fourier transform infrared data: Meteoritics & Planetary Science, v. 48, p. 2517–2530, https://doi.org/10.1111/maps.12223.

Greshake, A., Wirth, R., Fritz, J., Jakubowski, T., and Böttger, U., 2018, Mullite in Libyan Desert Glass: Evidence for high-temperature/low-pressure formation: Meteoritics & Planetary Science, v. 53, p. 467–481, https://doi.org/10.1111/maps.13030.

Kenny, G.G., Schmieder, M., Whitehouse, M.J., Nemchin, A.A., Morales, L.F.G., Buchner, E., Bellucci, J.J., and Snape, J.F., 2019, A new U-Pb age for shock-recrystallised zircon from the Lappajärvi impact crater, Finland, and implications for the accurate dating of impact events: Geochimica et Cosmochimica Acta, v. 245, p. 479–494, https://doi.org/10.1016/j.gca.2018.11.021.

Kleinmann, B., 1968, The breakdown of zircon observed in the Libyan Desert Glass as evidence of its impact origin: Earth and Planetary Science Letters, v. 5, p. 497–501, https://doi.org/10.1016/S0012-821X(68)80085-8.

Kleinmann, B., Horn, P., and Langenhorst, F., 2001, Evidence for shock metamorphism in sandstones from the Libyan Desert Glass strewn field: Meteoritics & Planetary Science, v. 36, p. 1277–1282, https://doi.org/10.1111/j.1945-5100.2001.tb01960.x.

Koeberl, C., 1997, Libyan Desert Glass: Geochemical composition and origin, *in* De Michele, V., ed., Proceedings of the Silica '96 Meeting on Libyan Desert Glass and Related Desert Events, Bologna: Milan, Italy, Pyramids, p. 121–131.

Koeberl, C., 2000, Confirmation of a meteoritic component in Libyan Desert Glass from osmium-isotopic data: Meteoritics & Planetary Science, v. 35, p. A89–A90.

Koeberl, C., and Ferrière, L., 2019, Libyan Desert Glass area in western Egypt: Shocked quartz in bedrock points to a possible deeply eroded impact structure in the region: Meteoritics & Planetary Science, https://doi.org/10.1111/maps.13250 (in press).

Kusaba, K., Syono, Y., Kikuchi, M., and Fukuoka, K., 1985, Shock behavior of zircon: Phase transition to scheelite structure and decomposition: Earth and Planetary Science Letters, v. 72, p. 433–439, https://doi.org/10.1016/0012-821X(85)90064-0.

Leroux, H., Reimold, W.U., Koeberl, C., Hornemann, U., and Doukhan, J.-C., 1999, Experimental shock deformation in zircon: A transmission electron microscopic study: Earth and Planetary Science Letters, v. 169, p. 291–301, https://doi.org/10.1016/S0012-821X(99)00082-5.

Rochette, P., et al., 2019, Pantasma: Evidence for a Pleistocene circa 14 km diameter impact crater in Nicaragua: Meteoritics & Planetary Science, v. 54, p. 880–901, https://doi.org/10.1111/maps.13244.

Schultz, P.H., Zárate, M., Hames, W.E., Harris, R.S., Bunch, T.E., Koeberl, C., Renne, P., and Wittke, J., 2006, The record of Miocene impacts in the Argentine Pampas: Meteoritics & Planetary Science, v. 41, p. 749–771, https://doi.org/10.1111/j.1945-5100.2006.tb00990.x.

Swamy, V., Saxena, S.K., Sundman, B., and Zhang, J., 1994, A thermodynamic assessment of silica phase diagram: Journal of Geophysical Research, v. 99, p. 11,787–11,794, https://doi.org/10.1029/93JB02968.

Timms, N.E., Erickson, T.M., Pearce, M.A., Cavosie, A.J., Schmieder, M., Tohver, E., Reddy, S.M., Zanetti, M.R., Nemchin, A.A., and Wittmann, A., 2017, A pressure-temperature phase diagram for zircon at extreme conditions: Earth-Science Reviews, v. 165, p. 185–202, https://doi.org/10.1016/j.earscirev.2016.12.008.

Walter, L.S., 1965, Coesite discovered in tektites: Science, v. 147, p. 1029–1032, https://doi.org/10.1126/science.147.3661.1029.

Wasson, J.T., 2003, Large aerial bursts: An important class of terrestrial accretionary events: Astrobiology, v. 3, p. 163–179, https://doi.org/10.1089/153110703321632499.

Printed in USA